Revista Ciência Agronômica, v. 56, e202392095, 2025
Centro de Ciências Agrárias - Universidade Federal do Ceará, Fortaleza, CE
www.ccarevista.ufc.br

Scientific Article
ISSN 1806-6690

VIS-NIR-SWIR spectroscopy in the evaluation nutritional status irrigated mango in the Brazilian semi-arid region[1]

Patrícia de Araujo Souza[2], Marcos Sales Rodrigues[3], Daniel dos Santos Costa[4], Kátia Araújo da Silva Rocha[2*], Augusto Miguel Nascimento Lima[3]

ABSTRACT - Leaf analysis is an important instrument that assists in the fertilization management of agricultural crops. However, the delay and high cost of conventional methods make its execution difficult. In this context, vis-NIR-SWIR (visible - near infrared - shortwave infrared) spectroscopy emerges as an analysis tool that is faster, more affordable and without major environmental impacts. Thus, the objective of this study was to quantify leaf macro and micronutrients in mango cv. Tommy Atkins cultivated under irrigation in the Brazilian semi-arid region with the use of vis-NIR-SWIR spectroscopy. 159 leaf samples of mango cv. Tommy Atkins coming from three distinct commercial areas were used. For these samples, the reflectance spectra were obtained for a spectral range from 350 to 2500 nm, and the contents of N, P, K, Ca, Mg, B, Zn, Fe, Mn and Cu were determined by the reference methods. Spectral data were initially subjected to preprocessing techniques. Then, multivariate regression models were developed. For all calibrated models, cross-validation was performed and for the models with better performance, external validation was performed. Regressive models had strong predictive performance for P and Ca ($R^2 > 0.70$), moderate for N and Zn ($0.50 < R^2 < 0.70$), weak for Fe ($0.30 < R^2 < 0.50$) and very weak for K, Mg, B, Cu and Mn ($R^2 < 0.30$). Therefore, vis-NIR-SWIR spectroscopy is a potential complementary tool to quantify the contents of these nutrients in mango cv. Tommy Atkins.

Key words: Fruit growing. Macronutrients. *Mangifera indica L*. Micronutrients. Proximal sensing.

DOI: 10.5935/1806-6690.20250061
Editor-in-Chief: Prof. Adriel Ferreira da Fonseca - adrielff@gmail.com
*Author for correspondence
Received for publication 05/09/2023; approved on 06/01/2025
[1]Extracted from the master's dissertation of the first author
[2]Federal University of São Francisco Valley, Agricultural Science Campus, Post-graduation Program of Agronomy - Vegetable Production, Petrolina-PE, Brazil, pathricia.4321.araujo@gmail.com (ORCID ID 0000-0002-0840-9543), katia_a.s@outlook.com (ORCID ID 0000-0001-6618-8753)
[3]Federal University of São Francisco Valley, Agricultural Science Campus, College of Agronomic Engineering, Petrolina-PE, Brazil, marcos.rodrigues@univasf.edu.br (ORCID ID 0000-0002-6567-1273), augusto.lima@univasf.edu.br (ORCID ID 0000-0002-8567-9600)
[4]Federal University of São Francisco Valley, College of Agricultural and Environmental Engineering, Juazeiro, Bahia, Brazil, daniel.costa@univasf.edu.br (ORCID ID 0000-0001-7703-3183)

INTRODUCTION

Mango (*Mangifera indica L.*) is among the main tropical fruit species cultivated in Brazil. The country is the third largest exporter of mango, which is one of the fruits with the highest added value in Brazilian exports. In this context, it is worth mentioning that the São Francisco Valley region is responsible for the production of almost all the mango exported by Brazil (Kist *et al*., 2022). Mango crop has a high nutritional requirement throughout its production cycle, so the practice of fertilization is essential for obtaining high fruit yields (Faria *et al*., 2016). Considering that leaf analysis complements soil analysis, characterization of plant nutritional status is very relevant, and in this perspective, leaf nutrient analysis is an important tool to optimize the fertilization process (Comino *et al*., 2018).

However, monitoring plant mineral nutrition during fruit development may require a number of complex chemical analyses of a large number of leaf samples, which is a very time-consuming and costly task, besides having an obviously negative environmental impact due to the production of harmful chemicals during analysis techniques (Galvez-Sola *et al*., 2015). In this context, the use of proximal sensing, with vis-NIR-SWIR (visible - near infrared - shortwave infrared) spectroscopy can help in the evaluation of the fertilization program because it is a faster, more economical and clean method of analyzing the structural and morphological characteristics of leaves (Rodrigues *et al*., 2020).

Prananto, Minasny and Weaver (2021) demonstrated the efficacy of near-infrared spectroscopy (NIRS) for analyzing nutrient content in cotton leaves. Their study developed predictive models using NIRS for key nutrients like nitrogen, phosphorus, and potassium. The results showed high accuracy, with R^2 values exceeding 0.85 for most nutrients, indicating strong correlations between spectral data and laboratory-measured concentrations. Similarly, Acosta *et al*. (2023) applied visible and near-infrared (Vis-NIR) spectroscopy to predict nutrient concentrations in citrus leaves. Their research focused on macro and micronutrients and achieved high prediction accuracies, with R^2 values above 0.80 for nutrients like nitrogen and magnesium. Therefore, these studies (Acosta *et al*., 2023; Prananto; Minasny; Weaver, 2021) and others have shown promising results with the use of vis-NIR-SWIR spectroscopy in the analysis of plant cell constituents such as chlorophyll, moisture and pigments (Liu *et al*., 2019; Wang *et al*., 2018) and leaf mineral nutrients in annual and perennial crops (Comino *et al*., 2018; Rodrigues *et al*., 2020).

Two widely used techniques in spectral data analysis for nutrient prediction were used, which are Partial Least Squares Regression (PLSR) and Multiple Linear Regression (MLR). PLSR is widely recognized for its ability to handle multicollinearity in spectral data and extract latent variables, making it a robust method for spectral analysis, especially in complex agricultural datasets (Wold; Sjöström; Eriksson, 2001). On the other hand, MLR is valued for its simplicity and interpretability, often serving as a baseline model for comparison in regression tasks (Martens; Næs, 1989).

Gill *et al*. (2024) demonstrated PLSR's ability to accurately profile macro and micronutrient concentrations in winter wheat using visible-to-shortwave infrared (VSWIR) spectroscopy. Similarly, Mahajan *et al*. (2021) highlighted PLSR's effectiveness in monitoring foliar nutrient status in mango trees, showcasing its adaptability across diverse crops and conditions. On the other hand, MLR serves as a simpler, interpretable baseline for regression analysis, making it a complementary tool to PLSR in studies requiring straightforward relationships between variables. While it may lack the robustness of PLSR in complex datasets, MLR provides valuable insights when applied to smaller datasets or when variable interactions are minimal.

Few studies have been reported regarding the quantitative determination of the contents of leaf macro and micronutrients in the mango crop, mainly under semi-arid conditions. The hypothesis of this study is that the leaf nutrient contents of the mango cv. Tommy Atkins are correlated with the spectra of the Vis-NIR-SWIR sensor, allowing their quantification in shorter time and at lower cost, hence enabling monitoring of the nutritional levels of the crop.

Therefore, the objective of this study was to quantify leaf macro and micronutrients in irrigated mango cv. Tommy Atkins in the Brazilian semi-arid region using vis-NIR-SWIR spectroscopy.

MATERIAL AND METHODS

Study area description and data collection

The leaf samples came from three commercial areas cultivated with irrigated mango cv. Tommy Atkins, located in the municipalities of Petrolina-PE and Juazeiro-BA, in the Sub-Middle São Francisco Valley, Brazilian semi-arid region (Table 1). The climate of the region, according to Köppen and Geiger classification, is BSh type – semi-arid hot. The average temperature is 32.7 ºC, the average relative humidity is 56.7%, the average annual precipitation is 373.3 mm distributed in four to five months during the year.

Table 1 - Location, relief, soil, area, crop age, crop spacing, irrigation and fertilization of the areas Barreiro de Santa Fé, Mandacaru and Sempre Verde cultivated with irrigated mango cv. Tommy Atkins in the Brazilian semi-arid region

	Area 1	Area 2	Area 3
Location	Barreiro de Santa Fé farm, Petrolina, Pernambuco (9°23'39.37" S and 40°44'32.91" W)	Mandacaru farm, Petrolina, Pernambuco (9°20'50.58" S and 40°33'04.51" W)	Sempre Verde farm, Juazeiro, Bahia (9°14'59.38" S and 40°16'58.40" W)
Relief	Flat	Flat	Flat
Soil	Oxisol	Ultisol	Ultisol
Area	9 ha (797 x 114 m)	4.5 ha (353 x 125 m)	9.5 ha (411 x 232 m)
Crop age	25 years	26 years	25 years
Crop spacing	8 x 5 m	8 x 5 m	7 x 5 m
Irrigation	Localized micro-sprinkler (2 micro-sprinklers/plant)	Localized micro-sprinkler (2 micro-sprinklers/plant)	Localized micro-sprinkler (2 micro-sprinklers/plant)
Fertilization	Via fertigation for N, P and K and manual application for Ca and Mg	Via fertigation for N, P and K and manual application for Ca and Mg	Via fertigation for N, P and K and manual application for Ca and Mg

Leaf samples were collected in the form of regular sampling grids after harvest (before application of inputs) in the areas of Barreiro de Santa Fé, Mandacaru and Sempre Verde farms, respectively, totaling 159 samples (Figure 1). Leaves were collected in the four quadrants of the plants and at the crown's middle third height, two leaves per quadrant of the last vegetative flushes (Genú; Pinto, 2002).

Reference analyses and descriptive statistics

The leaf samples were briefly washed with distilled water, then placed in paper bags and dried in an oven with forced air circulation at 60 ºC until reaching constant weight. Then, they were crushed in a stainless steel knife mill (Wiley type) to obtain particles with diameter of 0.85 mm. The leaf samples were subjected to wet digestion with sulfuric acid to determine N content (Kjeldahl distillation) and with nitric-perchloric solution to determine the contents of P (UV-Vis spectrophotometry), K (flame photometry), Ca, Mg, Fe, Zn, Cu, B and Mn (atomic absorption spectrometry), according to Silva (2009).

The data were subjected to descriptive analysis (mean, maximum, minimum, standard deviation and coefficient of variation (CV)) and their distributions were tested for normality using the Shapiro-Wilk test at 5% probability level. The CV was classified according to Pimentel-Gomes and Garcia (2002) as low (CV ≤ 10%), medium (10% < CV ≤ 20), high (20% < CV ≤ 30) and very high (CV > 30%). The classification proposed by Quaggio (1996) (Table 2) was also used to interpret the average leaf nutrient contents.

Acquisition of spectral data

Spectral data were obtained using 10 cm^3 of the samples of dried and crushed leaves. The reflectance spectra of the samples were obtained by: (1) a FieldSpec 3 spectroradiometer (*Analytical Spectral Devices*, Boulder, Colorado, USA), which has an optical sensor with 8° field of view, spectral range of 350 to 2500 nm, resolution of 8 nm, and precision of ± 1 nm; (2) 50-W quartz tungsten-halogen lamp; (3) dark chamber with dimensions of 100 × 50 x 50 cm; and (4) computer with RS3 software (*Analytical Spectral Devices*, Boulder, Colorado, USA). The fiber optic sensor was positioned perpendicular to the measurement plane, with a height of 7.0 cm, and the soil samples were placed in the center of this plane.

Blank reference consisted of a Spectralon ceramic plate (*Labsphere Inc.*, North Sutton, NH, USA), with which calibration operations were performed prior to data acquisition. Each spectrum of each leaf sample was composed of an average of 30 scans performed by the device. The reflectance values obtained were used to construct the mean spectral curves of the leaf samples. Subsequently, the reflectance values were transformed into absorbance values (log(1/R)), where R means reflectance, using the ViewSpec Pro software (*Analytic Spectral Devices*, Boulder, Colorado, USA). Absorbance data were used to construct predictive models.

Chemometric analyses

Chemometric analyses were performed using Unscrambler X 10.4 software (CAMO ASA, Oslo, Norway). Initially, spectral data were subjected to different pre-processing combinations. Smoothing with moving average filter (MAF) was applied to the spectral data in various segment sizes (7, 15, 25 and 35 points). The first and second derivatives of Savitzky-Golay, with second-order polynomial and various segment sizes (7, 15, 25 and 35 points), were applied to the smoothed data. Multiplicative scattering correction

Figure 1 - Location and distribution of sampling points in the areas Barreiro de Santa Fé, Mandacaru and Sempre Verde cultivated with irrigated mango cv. Tommy Atkins in the Brazilian semi-arid region

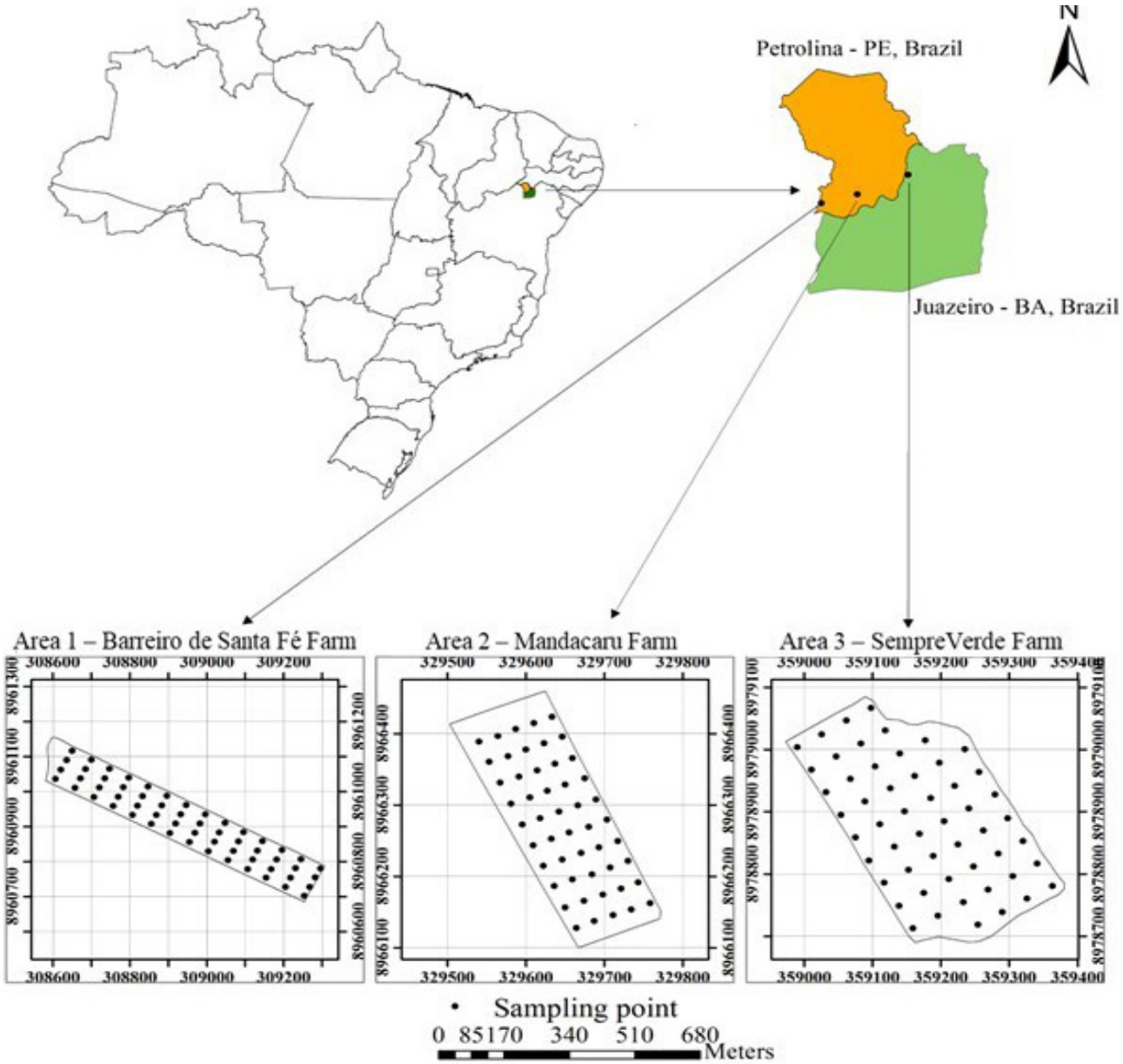

(MSC), standard normal variable (SNV) transformation, and orthogonal signal correction (OSC) were applied to the smoothed data and/or derivatives according to Ferreira (2015).

Predictive models to determine leaf nutrients were developed with partial least squares regression (PLSR). The data set was divided using the Kennard-Stone algorithm (Kennard; Stone, 1969), comprising 212 samples for calibration and cross-validation, and 106 samples for external validation. Preprocessed spectral data were used as predictor variables (X), and the contents of different leaf nutrients were used as response variables (Y). Also, spectral data were divided by regions, being modeled for Vis region (visible: 350-700 nm), NIR region (near infrared: 701-1300 nm), SWIR region (shortwave infrared: 1301-2500 nm), and Vis-NIR-SWIR region (350-2500 nm). The NIPALS algorithm (Geladi; Kowalski, 1986) with 100 iterations was used.

In order to solve the problems of collinearity of the data matrix and allow the development of predictive models with multiple linear regression (MLR), a selection

Table 2 - Adequate leaf nutrient contents for mango crop in the full flowering stage

Nutrients	Adequate range
N (g kg^{-1})	12.0 to 14.0
P (g kg^{-1})	0.8 to 1.6
K (g kg^{-1})	5.0 to 10.0
Ca (g kg^{-1})	20.0 to 35.0
Mg (g kg^{-1})	2.5 to 5.0
B (mg kg^{-1})	50 to 100
Zn (mg kg^{-1})	20 to 40
Fe (mg kg^{-1})	50 to 200
Cu (mg kg^{-1})	10 to 50
Mn (mg kg^{-1})	50 to 100

nd = not defined. Source: Quaggio (1996)

of variables of wavelengths was performed from the graphical analysis of the weights of spectral variables of leaf nutrients in the PLSR models. These selected wavelengths were used as predictor variables for the MLR models. After the construction of the MLR models, the selected variables were subjected to analysis of variance (ANOVA), and the models were reconstructed with the significant variables (*p-value* < 0.05).

The performance of the models was evaluated based on the statistical parameters: coefficient of determination (R^2); root mean square error of calibration (RMSEC); standard error of calibration (SEC); root mean square error of cross-validation (RMSECV); standard error of cross-validation (SECV); root mean square error of prediction (RMSEP); standard error of prediction (SEP); and bias. These parameters are defined by the following equations:

$$R^2 = \frac{\sum_{i=1}^{n}(\hat{y}_i - \bar{y})(y_i - \bar{y})^2}{(n-1)\sigma_r \sigma_p} \quad (1)$$

$$RMSEC = \sqrt{\frac{\sum_{n=1}^{n}(y_i - \hat{y}_i)^2}{n}} \quad (2)$$

$$SEC = \sqrt{\frac{n\ RMSEC^2}{n-1}} \quad (3)$$

$$RMSECV = \sqrt{\frac{\sum_{i=1}^{n}(y_i - \hat{y}_{i*})^2}{n}} \quad (4)$$

$$SECV = \sqrt{\frac{\sum_{i=1}^{n}(\hat{y}_i - y_i - bias)^2}{n-1}} \quad (5)$$

$$RMSEP = \sqrt{\frac{\sum_{i=1}^{n}(\hat{y}_i - y_i)^2}{m}} \quad (6)$$

$$SEP = \sqrt{\frac{\sum_{i=1}^{n}(\hat{y}_i - y_i - bias)^2}{m-1}} \quad (7)$$

$$bias = \frac{\sum_{i=1}^{n}(\hat{y}_i - y_i)}{m} \quad (8)$$

Where $\hat{y}_i$ is the value estimated by the calibration model; $\hat{y}_{i*}$ is the value estimated by the model in the cross-validation step; y_i is the reference value; $\bar{y}$ is the average of the reference values; $\bar{\hat{y}}$ is the average of the predicted values; *n* is the number of samples in the calibration or validation steps; *m* is the number of predicted samples; σ_r is the standard deviation of the reference values; σ_p is the standard deviation of the predicted values; and S_r^2 is the variation of the reference values.

The performance of the PLSR and MLR models was compared, and the prediction of leaf contents of nutrients was performed considering those that showed, simultaneously, lower values of standard error and higher values of coefficient of determination of calibration and cross-validation. For the selected models, external validation was performed. Finally, the classification proposed by Moore, Notz and Fligner (2015) was used, as follows: strong ($R^2 > 0.70$), moderate ($0.50 < R^2 < 0.70$), weak ($0.30 < R^2 < 0.50$) and very weak ($R^2 < 0.30$).

RESULTS AND DISCUSSION

Exploratory analysis of leaf nutrients and spectrum

Table 3 and 4 shows the descriptive statistics of leaf nutrient contents of irrigated mango cv. Tommy Atkins from the Barreiro de Santa Fé, Mandacaru and Sempre Verde areas.

Based on the values of coefficient of variation (CV), the leaf nutrient contents in the three areas showed medium to very high variability, according to Pimentel-Gomes and Garcia (2002). The presence of variation in the reference values allows the development of stable, widely applicable and highly robust predictive models.

The high variation of leaf nutrients may have occurred due to the uniform application of fertilizers in areas that showed spatial variability of soil attributes (Lira *et al.*, 2021), leading to a varied availability of nutrients in different locations, which consequently resulted in different absorption rates.

The nutrient analysis of mango tree leaves across three evaluated areas – Sempre Verde, Mandacaru, and Barreiro de Santa Fé revealed varying levels of adequacy, excess, and deficiency when compared to the reference table of Quaggio (1996) considereing the mean values. N levels were adequate in Mandacaru and Sempre Verde but deficient in Barreiro de Santa Fé. P was adequate in Barreiro de Santa Fé and Mandacaru, while K was adequate in all areas. Mg showed adequacy only in Mandacaru but was deficient in Barreiro de Santa Fé and Sempre Verde. B was adequate in Barreiro de Santa Fé and Sempre Verde but excessive in Mandacaru. Zn levels were adequate in Barreiro de Santa Fé and Mandacaru but deficient in Sempre Verde. Fe was adequate in Barreiro de Santa Fé and Sempre Verde but deficient in Mandacaru.

Mn levels were excessive across all areas, as were Ca levels. Cu was below adequate levels in all areas. These results highlight significant spatial variability in leaf nutrient status, emphasizing the need for tailored nutrient management strategies.

However, considering the maximum and minimum values the leaf contents of N, P and K (Table 3) ranged from deficient to excessive, those of Ca (Table 3) and B (Table 4) oscillated from adequate to excessive, those of Mg (Table 3), Zn and Cu (Table 4), ranged from deficient to adequate while those of Fe and Mn (Table 4) remained within the appropriate range considering the three areas evaluated. However, despite the content of these nutrients are below and above the adequate ranges, the plants showed no symptoms of deficiency or toxicity. Lira *et al*. (2021) observed that the nutritional sufficiency ranges established in the literature may not meet the nutritional requirement of irrigated mango in the semi-arid region, since most of the interpretation tables for macro and micronutrient contents were developed under different cultivation conditions and for expected yields lower than the average yield achieved in the São Francisco Valley.

The highest leaf contents were found for Ca in the three areas evaluated (Table 3). In the mango production system of the region, floral induction is commonly performed with the application of calcium and potassium nitrates, which can lead to the occurrence of high leaf Ca contents (Faria *et al*., 2016). The lower levels of K (Table 3) compared to Ca can be explained by the good mobility of K in the phloem and the considerable remobilization of this nutrient to the fruits, which are preferential sinks, during fruiting. In addition, K is the nutrient exported in largest quantity by the fruits, being associated with the quality parameters of mango (Tohidloo; Souri; Eskandarpour, 2018).

N is the main nutrient associated with vegetative growth, it is a constituent of the chlorophyll molecule and also of amino acids, and is correlated with protein levels. The main cellular phosphorus compounds are energy molecules, nucleic acids (DNA and RNA), phosphoproteins, phospholipids and sugar phosphates, in which phosphate groups are linked by a C–O–P bond (Bang *et al*., 2020).

Table 3 - Descriptive analysis of leaf macronutrient contents of irrigated mango cv. Tommy Atkins from the Barreiro de Santa Fé, Mandacaru and Sempre Verde areas cultivated in the Brazilian semi-arid region

Macronutrients	N	P	K	Ca	Mg
	g kg^{-1}				
Area 1 – Barreiro de Santa Fé farm					
Mean	7.82	1.14	9.00	41.55	2.26
Maximum	11.10	1.62	27.48	73.85	5.92
Minimum	3.22	0.74	2.25	23.06	1.55
CV (%)	19	19	65	41	30
CV classification	M	M	VH	VH	H
Area 2 – Mandacaru farm					
Mean	13.50	1.24	7.89	443.00	2.63
Maximum	17.78	1.94	22.50	547.96	3.54
Minimum	10.36	0.00	0.00	281.55	1.81
CV (%)	12	22	72	11	19
CV classification	M	H	VH	M	M
Area 3 – Sempre Verde farm					
Mean	12.12	3.28	5.92	92.55	2.46
Maximum	14.70	5.25	14.00	124.30	3.78
Minimum	3.50	2.21	1.59	48.38	1.14
CV (%)	16	21	55	25	25
Classification of CV	M	H	VH	H	H

Legend: Coefficient of variation (CV); Classification of CV according to Pimentel-Gomes and Garcia (2002): medium (M) = 10% < CV ≤ 20, high (H) = 20% < CV ≤ 30 and very high (VH) = CV > 30%

Table 4 - Descriptive analysis of leaf micronutrient contents of irrigated mango cv. Tommy Atkins from the Barreiro de Santa Fé, Mandacaru and Sempre Verde areas cultivated in the Brazilian semi-arid region

Micronutrients	B	Zn	Fe	Cu	Mn
	mg kg^{-1}				
	Area 1 – Barreiro de Santa Fé farm				
Mean	88.03	29.90	51.89	1.07	188.09
Maximum	162.52	62.77	168.41	5.21	348.26
Minimum	50.23	14.10	18.27	0.00	70.59
CV (%)	33	34	49	110	31
CV classification	VH	VH	VH	VH	VH
	Area 2 – Mandacaru farm				
Mean	132.79	24.94	38.37	4.25	158.25
Maximum	547.36	62.94	95.14	10.62	252.29
Minimum	27.24	4.48	22.74	2.37	93.40
CV (%)	52	64	33	33	22
CV classification	VH	VH	VH	VH	H
	Area 3 – Sempre Verde farm				
Mean	78.15	9.63	85.44	5.67	147.03
Maximum	148.69	34.85	169.86	12.47	856.30
Minimum	28.33	2.20	42.80	1.28	33.29
CV (%)	29	54	35	47	71
Classification of CV	H	VH	VH	VH	VH

Legend: Coefficient of variation (CV); Classification of CV according to Pimentel-Gomes and Garcia (2002): medium (M) = 10% < CV ≤ 20, high (H) = 20% < CV ≤ 30 and very high (VH) = CV > 30%

K is not a constituent of any plant molecule but participates in several physiological processes, acting as an activator of several enzymes, as a regulator of osmotic pressure and water regulator, in stimulating the assimilation and transport of assimilates and in the opening and closing of stomata, among other functions (Heikal, 2017).

Ca is a structural nutrient and is involved in supporting the cell wall structure. Mg is the central atom of the chlorophyll molecule. It also stabilizes cell membranes and is involved in the activation of several enzymes (Bang *et al*., 2020). B stimulates the growth of the pollen tube, the germination of the pollen grain and influences the metabolism and transport of carbohydrates (Muengkaew; Chaiprasarta; Wongsawad, 2017).

In addition, K and Ca contents are especially related to the quality attributes of mango fruits. The K provides an increase in the content of soluble solids, reduction of acidity, intensification of color and increase in vitamin content (Tohidloo; Souri; Eskandarpour, 2018). Ca provides firmness to mango fruits, delaying post-harvest softening and changes in texture during ripening (Muengkaew; Whangchai; Chaiprasart, 2018). The levels of N, P, K, and Mg, as well as N/Ca, K/Ca, and Mg/Ca ratios, play a crucial role in preventing physiological disorders in mango fruits, such as -internal flesh breakdown (Ma *et al*., 2022).

Figure 2 shows the spectral curves of average reflectance of leaf samples of irrigated mango cv. Tommy Atkins of the three areas evaluated. The lowest reflectance occurred in the range of 350 to 700 nm, with absorption peaks around 450 and 650 nm. The absorption at 450 nm was stronger than that at 650 nm. In the range of 700 to 770 nm, the reflection increased sharply and remained high up to 1332 nm. From 1332 to 2500 nm, there was a gradual decrease in leaf reflectance, with the presence of features in the spectral curves.

Reflectance in the range of 350 to 700 nm is associated with photosynthetically active radiation, so low reflection in this spectral region is due to strong absorption by photosynthetic pigments. Wavelengths around 450 and 650 nm correspond respectively to the blue and red bands of the electromagnetic spectrum. In the blue band there is absorption by chlorophylls and carotenoids, and in the red band there is absorption only by chlorophylls, so changes in leaf chlorophyll content lead to variations in the spectral data (Liu *et al*., 2019).

Figure 2 - Average reflectance spectra of leaf samples of irrigated mango cultivar Tommy Atkins in three production areas in the Brazilian semi-arid region

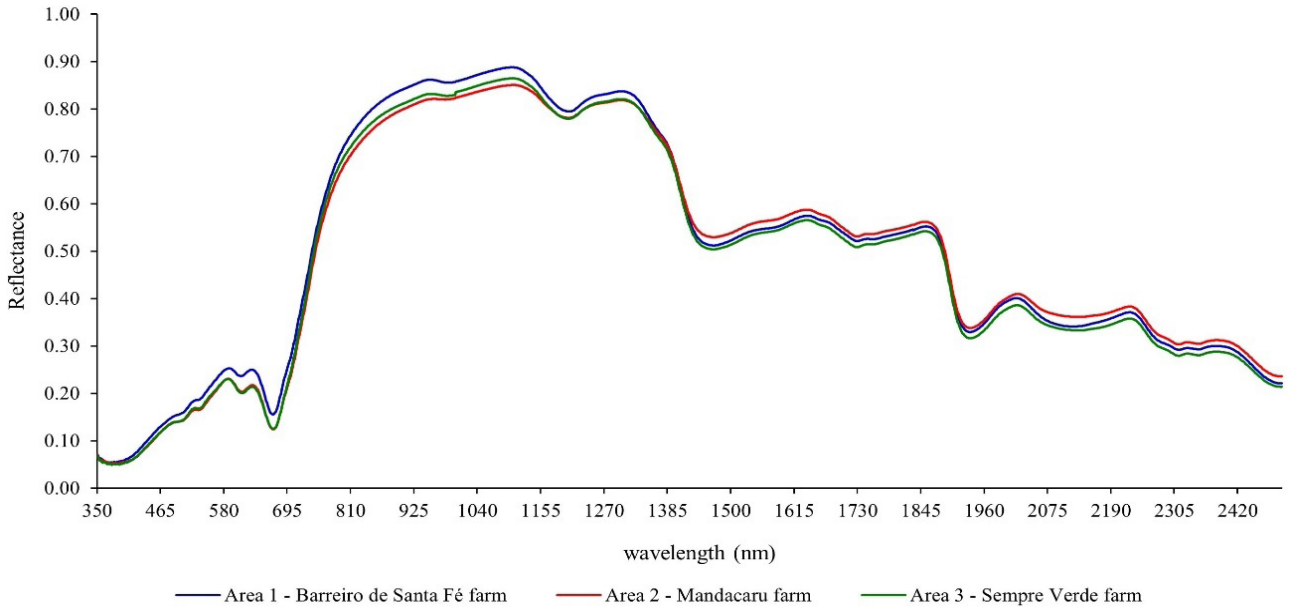

In the NIR region, there were no characteristics of strong absorption. This spectrum range contains information on leaf structure, and the high reflection in the NIR (near infrared) region occurs due to the multiple reflections caused by the scattering of light in the cellular arrangement. The SWIR (shortwave infrared) region shows several spectral signals caused by organic compounds that make up the dry matter in plant leaves such as carbohydrates, proteins and amino acids, among others (Peñuelas; Filella, 1998).

These compounds are used to indirectly quantify leaf nutrient levels, since mineral nutrients cannot be detected directly by vis-NIR-SWIR spectroscopy. For example, N is a constituent of chlorophyll and also of the amino acids that form proteins. K acts as an enzyme activator in the metabolism of proteins and carbohydrates. Mg is part of the ring structure of chlorophyll molecules and is associated with protein synthesis. These relationships allow the establishment of correlations between vis-NIR-SWIR spectra and foliar nutrients (Pandey *et al*., 2017). It was also observed that, among the three areas evaluated, area 1 had the lowest mean N content (Table 3) and also the highest mean reflectance in the visible region (Figure 2). For leaf samples from areas 2 and 3, there was greater absorption within this spectrum range.

Wang *et al*. (2018) observed in the tea species *Camellia sinensis L.* that an increase in the applied N dose caused an increase in leaf N contents and chlorophyll synthesis and led to a decrease in the values of reflectance in the visible range, which was associated with greater energy absorption by chlorophyll molecules.

Performance of chemometric models

Table 5 shows spectral signatures for the leaf nutrients of irrigated mango cv. Tommy Atkins. Zn and Mn had spectral signatures in the visible and NIR ranges, K had its most responsive wavelengths at the end of the spectral curve, while the other nutrients had spectral signatures along the entire vis-NIR-SWIR spectrum.

Figures 3, 4 and 5 presents the regression graphs and the performance parameters of the predictive models for leaf nutrients of irrigated mango cv. Tommy Atkins using vis-NIR-SWIR spectroscopy. The preprocessing that achieved the best predictive performance was OSC.

For K, the PLSR model had the best predictive performance, using the SWIR spectral region. For the other nutrients, the MLR model achieved the best predictive performance, using spectral signatures. According to the classification of Moore, Notz and Fligner (2015), considering the result of external validation, the fitted predictive models had strong performance for P and Ca, moderate performance for N and Zn, weak for Fe, and very weak for K, Mg, B, Cu and Mn.

Table 5 - Spectral signatures of leaf nutrients of irrigated mango cv. Tommy Atkins in the Brazilian semi-arid region

Nutrient	Wavelength (nm)
N (g kg^{-1})	432; 479; 509; 762; 1921; 2053; 2093 and 2100.
P (g kg^{-1})	499; 520; 565; 582; 617; 630; 673; 746; 1722 and 2306.
K (g kg^{-1})	1867; 1903; 2101; 2369; 2426 and 2477.
Ca (g kg^{-1})	614; 675; 1198; 1904; 2106 and 2330.
Mg (g kg^{-1})	494; 665; 1907; 1917; 1985; 1991; 2006; 2029; 2116; 2217; 2260; 2282; 2311; 2326; 2370 and 2381.
B (mg kg^{-1})	548; 647; 649; 669 and 2002.
Fe (mg kg^{-1})	521; 537; 631; 664; 1453; 2012; 2116 and 2276.
Zn (mg kg^{-1})	524; 551; 568; 673; 678; 716; 726 and 745.
Cu (mg kg^{-1})	474; 506; 520; 539; 564;580; 588; 617; 633; 674; 765; 1406; 1715; 1967; 2103 and 2305.
Mn (mg kg^{-1})	474; 502; 507; 522; 536; 582; 614; 632; 671; 752 and 777.

For all nutrients, it was observed that the selection of specific regions of the spectrum or spectral signatures led to the calibration of models with greater predictive capacity compared to the full spectrum. The selection of wavelengths for quantifying leaf nutrients was important because it reduces redundant information in the vis-NIR-SWIR spectra, optimizing the performance of predictive models (Malmir *et al*., 2019).

Leaf nutrients cannot be detected directly by vis-NIR-SWIR spectroscopy, but organic compounds of the leaf containing these elements – such as pigments, proteins and carbohydrates, among others – due to their C–H, O–H and N–H bonds, are spectrally active and can therefore be used to quantitatively and indirectly predict leaf nutrients (Wang *et al*., 2018).

Related spectral characteristics chlorophyll absorption, can characterize the N status of the leaves given that chlorophyll concentration is directly related to N content (Peñuelas; Filella, 1998). The wavelengths between the regions of 700 and 770 nm are in the transition between red and infrared, and the position of the red edge can also be used to predict chlorophyll concentration, which is related to N content (Malmir *et al*., 2019).

The reflectance spectrum in SWIR can also be a good indicator of leaf N content because to overtones and combinations of vibrational modes associated with the N–H and C–H bonds present in the amino acids and the C–H bonds of chlorophyll molecules (Curran, 1989).

The prediction of N using vis-NIR-SWIR spectroscopy was also moderate for oil palm leaves (Khorramnia *et al*., 2014). However, models with good prediction have been reported in studies with leaves of rapeseed (Zhang *et al*., 2013), soybean and maize (Pandey *et al*., 2017).

The amplitude of the data used to calibrate regressive models plays an important role in improving prediction accuracy. The range of N contents of this study (3.22 to 17.78 g kg^{-1}) had a lower amplitude than those reported in other studies (15.00 to 45.00 g kg^{-1}) (Pandey *et al*., 2017), which may have compromised the predictive capacity of the regressive model developed for N. Thus, the use of leaf samples from other phenological stages of mango crop may need to be considered in future studies in order to obtain a greater variation of leaf N content and thus improve the predictability of N from vis-NIR-SWIR spectra.

P is present in the ATP molecule (Adenosine triphosphate) and is therefore directly associated with physiological processes that require energy such as photosynthesis, so spectral information in the visible range can collaborate with the prediction of leaf P content. In addition, within plants, P is related to plant metabolic processes, and the SWIR band can be used to spectrally associate P contents with proteins, sugars and starches as representative end products of metabolism (Siedliska *et al*., 2021).

P was also predicted with good accuracy using vis-NIR-SWIR spectroscopy in leaves of rapeseed (Zhang *et al*., 2013), soybean and maize (Pandey *et al*., 2017). The leaf content range of this study (0.00 to 5.25 g kg^{-1}) had a greater amplitude compared to those reported in other studies (2.00 to 4.00 g kg^{-1}) (Pandey *et al*., 2017), which may have led to the calibration of a regressive model with strong prediction performance for P.

The spectral range between 1800 and 2100 nm is associated with the absorption of sucrose and other carbohydrates (Rébufa; Pany; Bombarda, 2018). The prediction of K content is due to the relationship of K with carbohydrates and organic acids. K influences photosynthesis and translocation of assimilates such as sucrose, cellulose and starch, so the abundance of these assimilates and organic acids, can be indirectly correlated with K content in plants (Bang *et al*., 2020).

Figure 3 - Performance N calibration (A), N cross-validation (B), N external validation (C), P calibration (D), P cross-validation (E), P external validation (F), K calibration (G), K cross-validation (H), K external validation (I) and Ca calibration (J) and parameters of the predictive models Partial Least Squares Regression (PSLR); Multiple linear regression (MLR); Coefficient of determination (R^2); Root mean square error of calibration (RMSEC); Standard error of calibration (SEC); Root mean square error of cross-validation (RMSECV); Standard error of cross-validation (SECV); Root mean square error of prediction (RMSEP); Standard error of prediction (SEP)

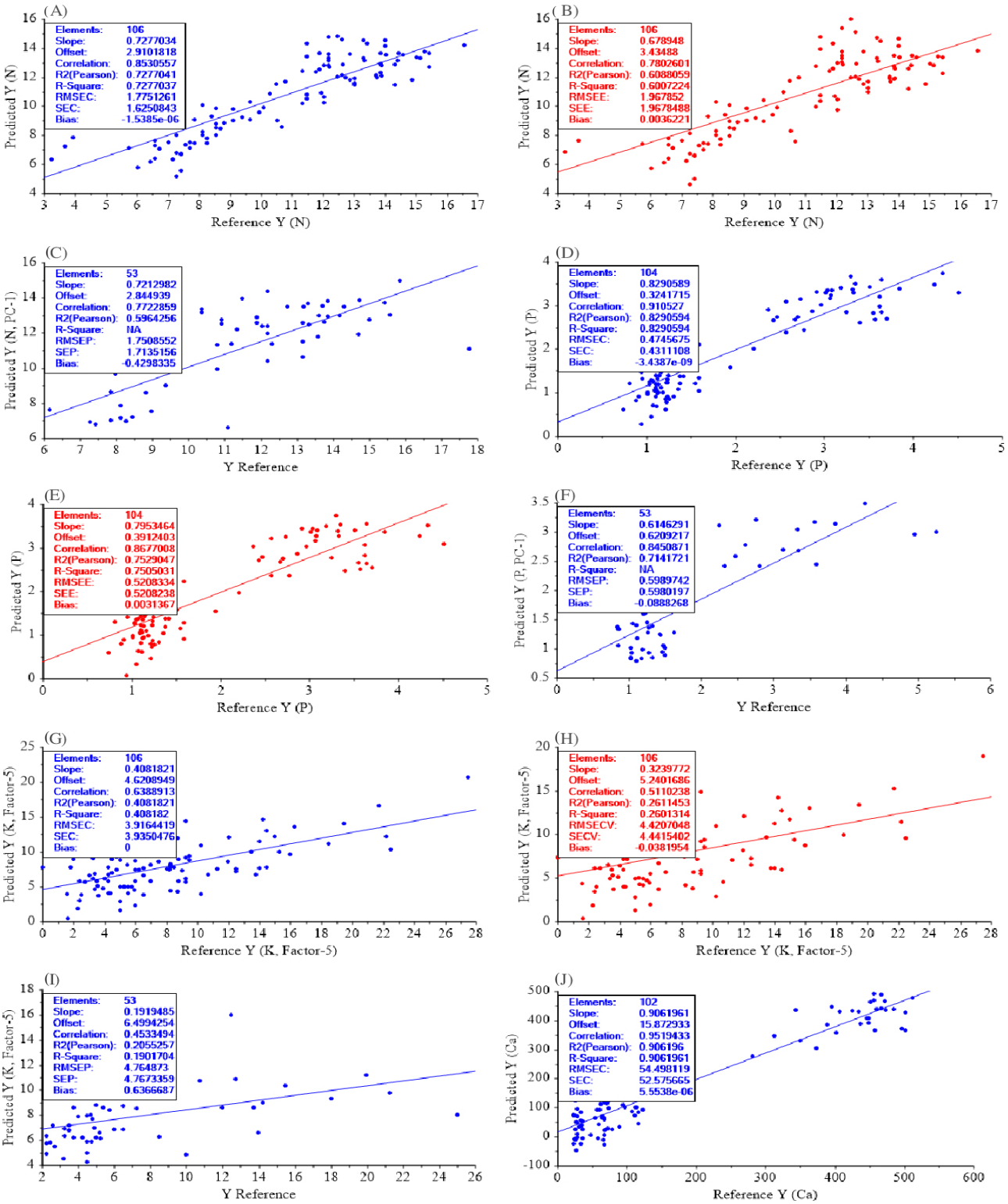

Figure 4 - Performance Ca cross-validation (A), Ca external validation (B), Mg calibration (C), Mg cross-validation (D), Mg external validation (E), B calibration (F), B cross-validation (G), B external validation (H), Zn calibration (I) and Zn cross-validation (J) and parameters of the predictive models Partial Least Squares Regression (PSLR); Multiple linear regression (MLR); Coefficient of determination (R^2); Root mean square error of calibration (RMSEC); Standard error of calibration (SEC); Root mean square error of cross-validation (RMSECV); Standard error of cross-validation (SECV); Root mean square error of prediction (RMSEP); Standard error of prediction (SEP)

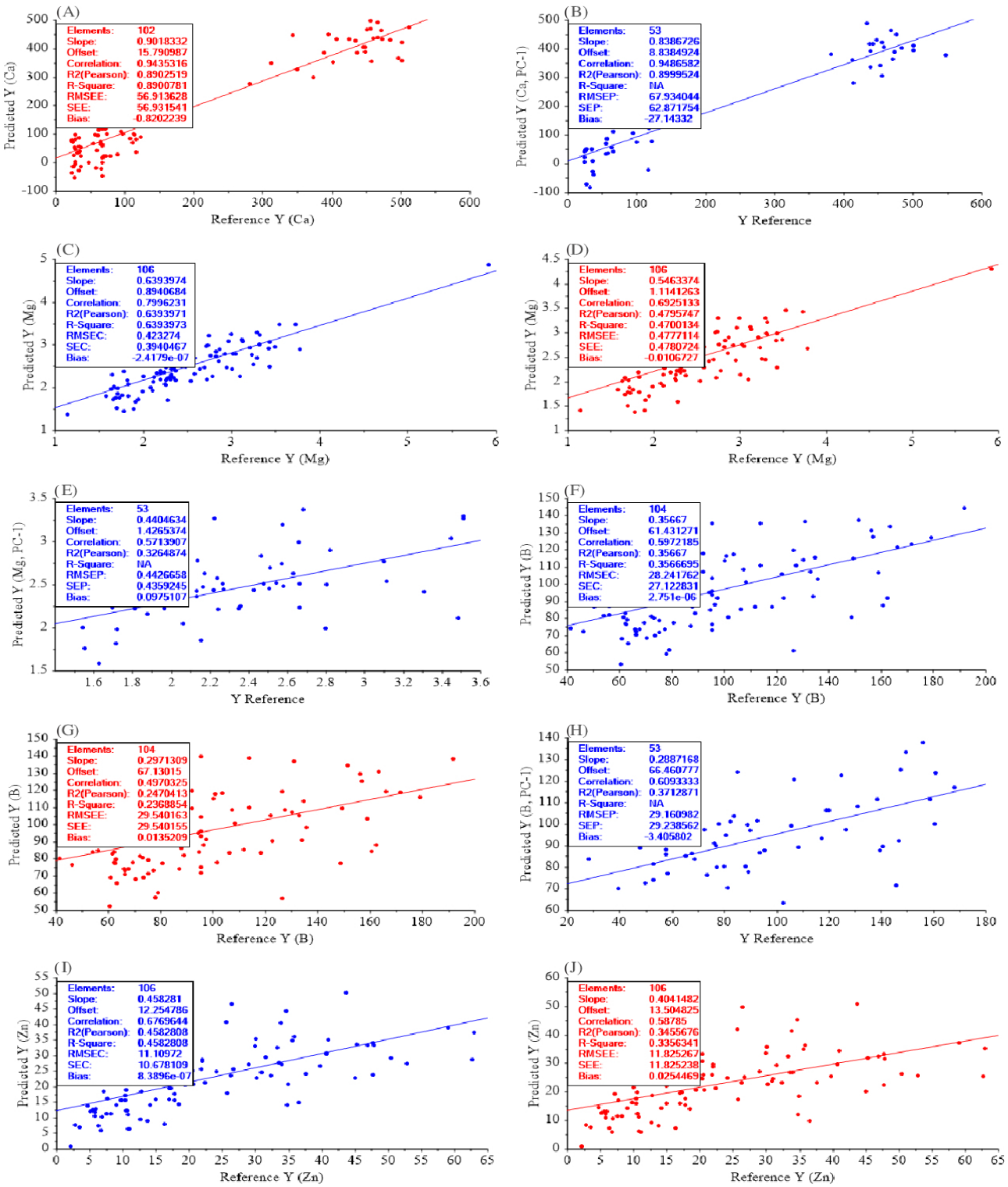

Figure 5 - Performance Zn external validation (A), Fe calibration (B), Fe cross-validation (C), Fe external validation (D), Cu calibration (E), Cu cross-validation (F), Cu external validation (G), Mn calibration (H), Mn cross-validation (I) and Mn external validation (J) and parameters of the predictive models Partial Least Squares Regression (PSLR); Multiple linear regression (MLR); Coefficient of determination (R^2); Root mean square error of calibration (RMSEC); Standard error of calibration (SEC); Root mean square error of cross-validation (RMSECV); Standard error of cross-validation (SECV); Root mean square error of prediction (RMSEP); Standard error of prediction (SEP)

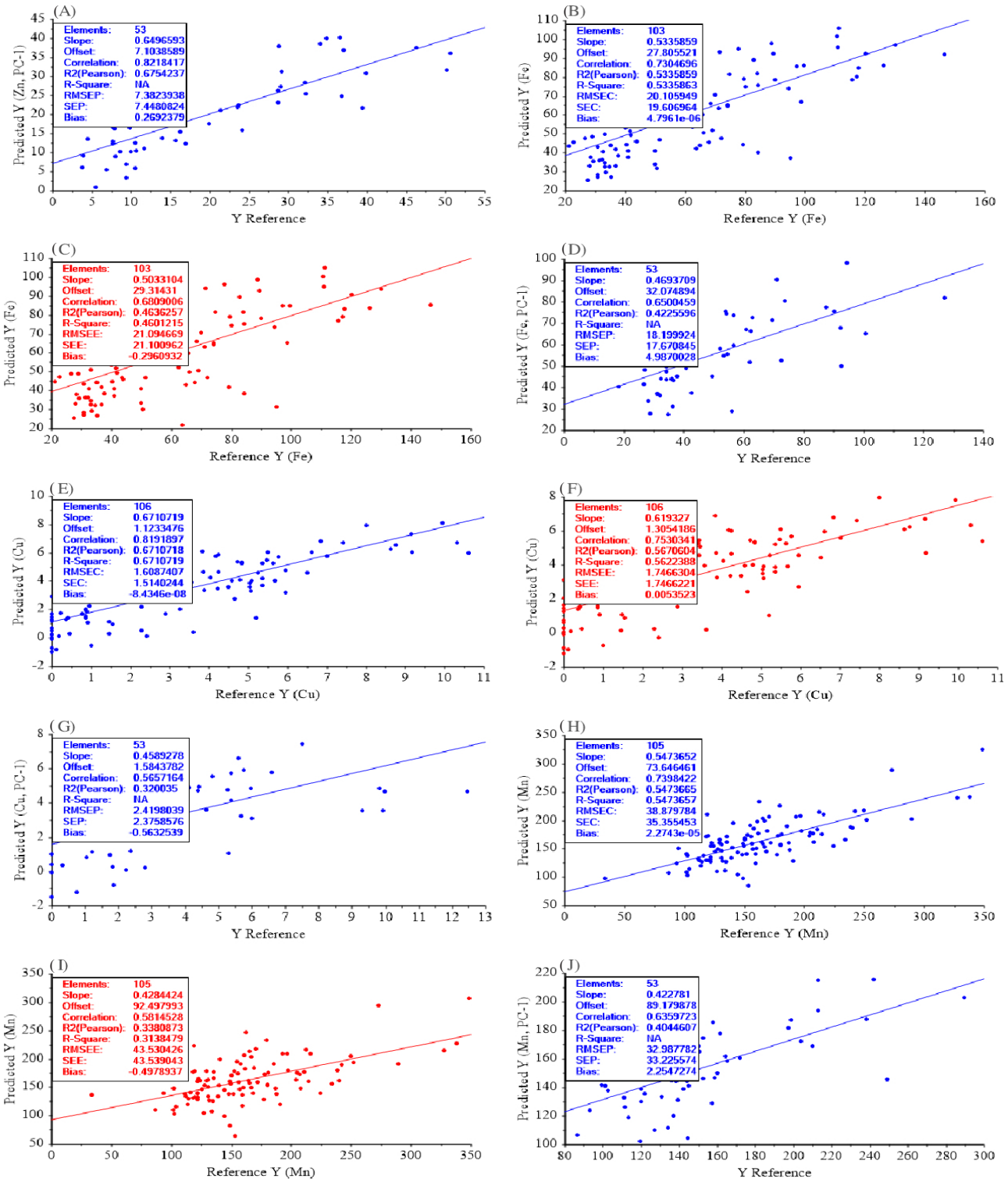

K was also not predicted with reliable performance in cacao leaves with vis-NIR-SWIR spectroscopy (Malmir *et al*., 2019), but had good prediction performance in leaves of rapeseed (Zhang *et al*., 2013), soybean and maize (Pandey *et al*., 2017). The leaf K content range of this study (0.00 to 27.48 g kg^{-1}) is close to the range reported by other studies (6.00 to 31.00 g kg^{-1}) (Pandey *et al*. 2017; Zhang *et al*. 2013), so the range of variation of the data was probably not a problem.

K acts as an osmotic regulator, being important in the absorption of water by plants, so leaf K content is generally highly correlated with leaf water content (Bang *et al*., 2020). Thus, the use of fresh leaf samples may need to be considered to improve the predictability of K in future studies.

Ca acts as a cofactor in photosystem II, so photosynthetically active radiation contributes to its prediction. The sensitivity of NIR characteristics to Ca is related to the cell structure of the leaf, since Ca is also a structural element that confers rigidity to the cell wall and integrity to the plasma membrane. Wavelengths in the SWIR region related to starch and amino acid absorption may also contribute to leaf Ca predictive models (Bang *et al*., 2020).

Ca has also been reliably predicted using vis-NIR-SWIR spectroscopy in leaves of olive (Comino *et al*., 2018), citrus (Galvez-Sola *et al*., 2015) and cacao (Malmir *et al*., 2019). The range of Ca contents of this study had a higher amplitude (23.06 to 547.96 g kg^{-1}) than that of other similar studies (0.89 to 6.77 g kg^{-1}) (Galvez-Sola *et al*., 2015), which may have contributed to the development of a model with strong prediction performance for leaf Ca.

Mg is the central element of the chlorophyll molecule (Bang *et al*., 2020), so chlorophyll-sensitive spectral characteristics, comprised in the visible range, contribute to the prediction of Mg (Liu *et al*., 2019). Spectral characteristics of SWIR around 2060, 2130, 2240, 2300 and 2350 nm are related to energy absorption by proteins (Curran, 1989). Spectral signatures close to protein-responsive wavelengths may contribute to the prediction of leaf Mg, since this nutrient is a bridging element for aggregation between ribosomal subunits, an essential process in protein synthesis, besides being an activator of some enzymes in plants (Bang *et al*., 2020).

Similar to the results found in this study, Comino *et al*. (2018) also observed regressive models with low prediction accuracy for Mg in olive leaves. However, Pandey *et al*. (2017) found moderate results in the prediction of Mg in soybean and maize leaves. The range of variation in the Mg contents of this study (1.14 to 5.92 g kg^{-1}) was close to those reported in other studies (5.00 to 7.00 g kg^{-1}) (Pandey *et al*., 2017), so the range of the data probably did not constitute a problem in the calibration of the model. Thus, the prediction of leaf Mg with vis-NIR-SWIR spectroscopy will need further future investigations for the development of satisfactory predictive models in mango crop.

Regarding micronutrients, some studies have shown that predictive models generally show lower performance compared to those of macronutrients (Comino *et al*., 2018). The vis-NIR-SWIR prediction of micronutrients may be compromised mainly by their low contents in the leaves (Galvez-Sola *et al*., 2015). However, for the micronutrient Zn, Rodrigues *et al*. (2020) also developed a regressive model of moderate prediction in soybean crop, similar to the results found in the present study. Zn is used in the process of chlorophyll biosynthesis and can therefore be related to wavelengths in the visible region (Zhang *et al*., 2019).

Despite some limitations, this study demonstrates the potential use of vis-NIR-SWIR spectroscopy to quantify leaf nutrients in the mango crop cv. Tommy Atkins, which showed R^2 above 0.50, as was the case of Ca, P, N and Zn, with the first two standing out with R^2 higher than 0.70.

Nutrients must be at the appropriate levels to achieve quality fruit production. In the mango crop for example, N should be high especially in the vegetative growth, panicle development and fruit growth stages. In addition, this nutrient has a maximum limit (14 g kg^{-1}) in the floral induction stage, and should not exceed this value (Silber *et al*., 2022).

Ca contents should be high mainly in the vegetative growth, flower development and fruit development stages. In addition, special attention should be paid to the Ca/N ratio in the leaf in order to avoid the occurrence of physiological disorders such as internal collapse (Bibi *et al*., 2019). P is normally supplied at the beginning of the production cycle and at flowering, and the highest leaf contents of this nutrient occur in the flowering and fruiting stages (Faria *et al*., 2016). Zn, in turn, shows peaks of leaf content before flowering and during fruit development (Mahida *et al*., 2018).

The proposed strategy introduces a significant innovation for scientific and technological development in the Brazilian semi-arid region by applying vis-NIR-SWIR spectroscopy to evaluate the nutritional status of irrigated mango crops. This method offers a rapid, cost-effective, and environmentally sustainable alternative to conventional nutrient analysis, enabling precise and real-time nutrient monitoring. By reducing the reliance on chemical analyses, it not only minimizes environmental impacts but also provides a scalable solution for enhancing fertilization management in mango production. The integration of this technology has the potential to revolutionize agricultural practices in the region, promoting precision agriculture and optimizing resource use to achieve higher yields and better fruit quality.

Therefore, vis-NIR-SWIR spectroscopy can help in the fertilization program of the aforementioned nutrients, considering that a rapid prediction of leaf nutrient content is of great importance to evaluate the nutritional status of the plant, enabling the adoption of a more adequate management of fertilizers in the mango crop.

CONCLUSIONS

Specific wavelengths of the vis-NIR-SWIR spectrum were shown to be sensitive to leaf contents of N, P, Ca and Zn in mango cv. Tommy Atkins grown under irrigation in the Brazilian semi-arid region. Thus, the prediction of P and Ca contents is strong ($R^2 > 0.70$), while the prediction of N and Zn contents is moderate ($0.70 > R^2 > 0.50$) with the use of proximal sensing. Therefore, vis-NIR-SWIR spectroscopy proved to be a viable tool to complement conventional analyses of leaf nutrient quantification, facilitating the assessment of the nutritional status of mango due to its speed and lower cost. Thus, this technology has the potential for application in agricultural management models with precision fruit growing.

ACKNOWLEDGMENTS

This study was financially supported by the CAPES Foundation, Ministry of Education of Brazil, Brasília, through the scholarship granted to the first author.

REFERENCES

ACOSTA, M. *et al*. Rapid prediction of nutrient concentration in citrus leaves using Vis-NIR spectroscopy. **Sensors**, v. 23, n. 14, p. 6530, 2023.

BANG, T. C. *et al*. The molecular-physiological functions of mineral macronutrients and their consequences for deficiency symptoms in plants. **New Phytologist**, v. 229, n. 5, p. 2446-2469, 2020.

BIBI, F. *et al*. Effect of foliar application of boron with calcium and potassium on quality and yield of mango cv. Summer Bahisht (SB) chaunsa. **Open Agriculture**, v. 4, n. 1, p. 98-106, 2019.

COMINO, F. *et al.* Near-infrared spectroscopy and X-ray fluorescence data fusion for olive leaf analysis and crop nutritional status determination. **Talanta**, v. 188, p. 676-684, 2018.

CURRAN, P. J. Remote sensing of foliar chemistry. **Remote Sensing of Environment**, v. 30, n. 3, p. 271-278, 1989.

FARIA, L. N. *et al*. Nutrient contents in 'Tommy Atkins' mango leaves at flowering and fruiting stages. **Engenharia Agrícola**, v. 36, n. 6, p. 1073-1085, 2016.

FERREIRA, M. M. C. **Quimiometria**: conceitos, métodos e aplicações. 2. ed. Campinas: Editora da Unicamp, 2015. 496 p.

GALVEZ-SOLA, L. *et al*. Rapid estimation of nutritional elements on citrus leaves by near infrared reflectance spectroscopy. **Frontiers in Plant Science**, v. 6, p. 1-8, 2015.

GELADI, P.; KOWALSKI, B. R. Partial least-squares regression: a tutorial. **Analytica Chimica Acta**, v. 185, p. 1-17, 1986.

GENÚ, P. J. C.; PINTO, A. C. Q. **A cultura da mangueira**. 1. ed. Brasília: Embrapa Informação Tecnológica, 2002. 452 p.

GILL, A. K. *et al*. Utilizing VSWIR spectroscopy for macronutrient and micronutrient profiling in winter wheat. **Frontiers in Plant Science**, v. 15, p. 1426077, 2024.

HEIKAL, A. A. M. The influence of foliar application of biostimulant atonik and different sources of potassium on full sun and partial shade *Salvia farinacea* plants. **Egyptian Journal Horticulture**, v. 44, n. 1, p. 105-117, 2017.

KENNARD, R. W.; STONE, L. A. Computer aided design of experiments. **Technometrics**, v. 11, n. 1, p. 137-148, 1969.

KHORRAMNIA, K. *et al*. Oil palm leaf nutrient estimation by optical sensing techniques. **Transactions of the ASABE**, v. 57, n. 4, p. 1267-1277, 2014.

KIST, B. B. *et al*. **Anuário brasileiro da fruticultura 2022**. 1. ed. Santa Cruz do Sul: Gazeta Santa Cruz, 2022. 96 p.

LIRA, A. L. F. *et al*. Spatial correlation between soil and leaf macronutrients in semiarid Brazilian mango (*Mangifera indica* L.) fields. **Revista Brasileira de Fruticultura**, v. 43, n. 4, p. 1-17, 2021.

LIU, J. *et al*. Nondestructive detection of rape leaf chlorophyll level based on Vis-NIR spectroscopy. Spectrochim. **Spectrochimica Acta Part A: Molecular and Biomolecular Spectroscopy**, v. 222, p. 1-7, 2019.

MA, X. *et al*. The link between mineral elements variation and internal flesh breakdown of 'Keitt' mango in a steep slope mountain area, southwest China. **Horticulturae**, v. 8, n. 6, p. 533-546, 2022.

MAHAJAN, G. R. *et al*. Monitoring the foliar nutrients status of mango using spectroscopy-based spectral indices and PLSR-combined machine learning models. **Remote Sensing**, v. 13, n. 4, p. 641, 2021.

MAHIDA, A. *et al*. Effect of Fe and Zn fertilization on fruit setting and yield attributes of mango cv. Kesar. **International Journal of Chemical Studies**, v. 6, n. 5, p. 532-534, 2018.

MALMIR, M. *et al*. Prediction of macronutrients in plant leaves using chemometric analysis and wavelength selection. **Journal of Soils and Sediments**, v. 20, n. 1, p. 249-259, 2019.

MARTENS, H.; NÆS, T. **Multivariate calibration**. Chichester: Wiley, 1989.

MOORE, D. S.; NOTZ, W. I.; FLIGNER, M. A. **The basic practice of statistics**. 7. ed. New York: WH Freeman, 2015. 774 p.

MUENGKAEW, R.; CHAIPRASARTA, P.; WONGSAWAD, P. Calcium-boron addition promotes pollen germination and fruit set of mango. **International Journal of Fruit Science**, v. 17, n. 2, p. 147-158, 2017.

PANDEY, P. *et al*. High throughput in vivo analysis of plant leaf chemical properties using hyperspectral imaging. **Frontiers in Plant Science**, v. 8, p. 1-12, 2017.

PEÑUELAS, J.; FILELLA, I. Visible and near-infrared reflectance techniques for diagnosing plant physiological status. **Trends in Plant Science**, v. 3, n. 4, p. 151-156, 1998.

PIMENTEL-GOMES, F.; GARCIA, C. H. **Estatística aplicada a experimentos agronômicos e florestais**: exposição com exemplos e orientações para uso de aplicativos. 1. ed. Piracicaba: FEALQ, 2002. 309 p.

PRANANTO, J. A.; MINASNY, B.; WEAVER, T. Rapid and cost-effective nutrient content analysis of cotton leaves using near-infrared spectroscopy (NIRS). **PeerJ**, v. 9, e11042, 2021.

QUAGGIO, J. A. Adubação e calagem para mangueira e qualidade dos frutos. *In:* SÃO JOSÉ, A. R. *et al*. **Manga tecnologia de produção e mercado**. 1. ed. Vitória da Conquista: DBZ/UESB, 1996. cap. 5, p. 106-135.

RÉBUFA, C.; PANY, I.; BOMBARDA, I. NIR spectroscopy for the quality control of Moringa oleifera (Lam.) leaf powders: prediction of minerals, protein and moisture contents. **Food Chemistry**, v. 261, p. 311-321, 2018.

RODRIGUES, M. *et al*. Vis–NIR spectroscopy: from leaf dry mass production estimate to the prediction of macro- and micronutrients in soybean crops. **Journal of Applied Remote Sensing**, v. 14, n. 4, p. 1-20, 2020.

SIEDLISKA, A. *et al*. Identification of plant leaf phosphorus content at different growth stages based on hyperspectral reflectance. **BMC Plant Biology**, v. 21, n. 28, p. 1-17, 2021.

SILBER, A. *et al*. Nitrogen uptake and macronutrients distribution in mango (*Mangifera indica L*. cv. Keitt) trees. **Plant Physiology and Biochemistry**, v. 181, p. 23-32, 2022.

SILVA, F. C. S. **Manual de análises químicas de solos, plantas e fertilizantes**. 2. ed. Brasília: Embrapa Informação Tecnológica, 2009. 628 p.

TOHIDLOO, G.; SOURI, M. K.; ESKANDARPOUR, S. Growth and fruit biochemical characteristics of three strawberry genotypes under different potassium concentrations of nutrient solution. **Open Agriculture**, v. 3, n. 1, p. 356-362, 2018.

WANG, Y. *et al*. Rapid prediction of chlorophylls and carotenoids content in tea leaves under different levels of nitrogen application based on hyperspectral imaging. **Journal of the Science of Food and Agriculture**, v. 99, n. 4, p. 1997-2004, 2018.

WOLD, S.; SJÖSTRÖM, M.; ERIKSSON, L. PLS-regression: a basic tool of chemometrics. **Chemometrics and Intelligent Laboratory Systems**, v. 58, n. 2, p. 109-130, 2001.

ZHANG, X. *et al*. Detecting macronutrients content and distribution in oilseed rape leaves based on hyperspectral imaging. **Biosystems Engineering**, v. 115, n. 1, p. 56-65, 2013.

ZHANG, J. *et al*. Transcriptomic and proteomic analyses reveal new insight into chlorophyll synthesis and chloroplast structure of maize leaves under zinc deficiency stress. **Journal of Proteomics**, v. 199, p. 123-134, 2019.